Proceedings of the
Annual Stability Conference
Structural Stability Research Council
Grapevine, Texas, April 18-21, 2012

Influence of weak-axis flexural yielding on strong-axis buckling strength of wide flange columns

C.D. Stoakes[1], L.A. Fahnestock[2]

Abstract
In multitier braced frames, the columns are typically wide flange sections with the weak axis oriented in the plane of the frame. Weak-axis buckling strength is commonly computed using an effective length equal to the tier height and the strong-axis buckling strength is based on an effective length equal to the total height of the braced frame. During a large seismic event, inelasticity in the braces can result in differential tier drifts that induce weak-axis flexural yielding of the columns. This inelasticity is not considered in current column strength curves. As a first step toward quantifying the influence of weak-axis flexural yielding on strong-axis buckling strength of wide flange columns, several representative isolated columns were subjected to compressive loads in combination with varying levels of weak-axis flexural yielding using three-dimensional finite element analysis. The results from the computational studies suggest that strong-axis buckling strength can be significantly degraded due to the presence of weak-axis flexure if the weak-axis rotation is large and torsional restraint is not provided at the tier levels.

1. Background

Multitier braced frames are used in many types of construction, including tall industrial buildings, performing-arts centers, stadiums, and convention centers. A multitier braced frame is created when a braced frame with a large aspect ratio is subdivided into a series of braced tiers with intermediate beams. The columns are not braced in the out-of-plane direction at the tier levels, however. Typically, wide flange shapes with weak axis oriented in the plane of the frame are used for the braced frame columns. In current design practice, the weak-axis buckling strength is computed using an effective length equal to the tier height, h, and the strong-axis buckling strength is based on an effective length equal to the total height of the braced frame, H. The representative multitier braced frame shown in Fig. 1 (Sabelli 2011) has four tiers with $H = 4h$.

During a large seismic event, brace inelasticity can result in differential tier drifts that induce weak-axis flexural yielding of the braced frame columns. The current column strength curve in

[1] Lecturer, University of Iowa, <christopher-stoakes@uiowa.edu>
[2] Assistant Professor, University of Illinois at Urbana-Champaign, <fhnstck@illinois.edu>

the AISC *Specification for Structural Steel Buildings* (AISC 2005c) does not account for the effect of this inelasticity on the strong-axis buckling strength of the column. Fig. 1a shows an example multitier braced frame and Fig. 1b shows the deformed shape of the structure after in-plane flexural yielding in the braced frame columns.

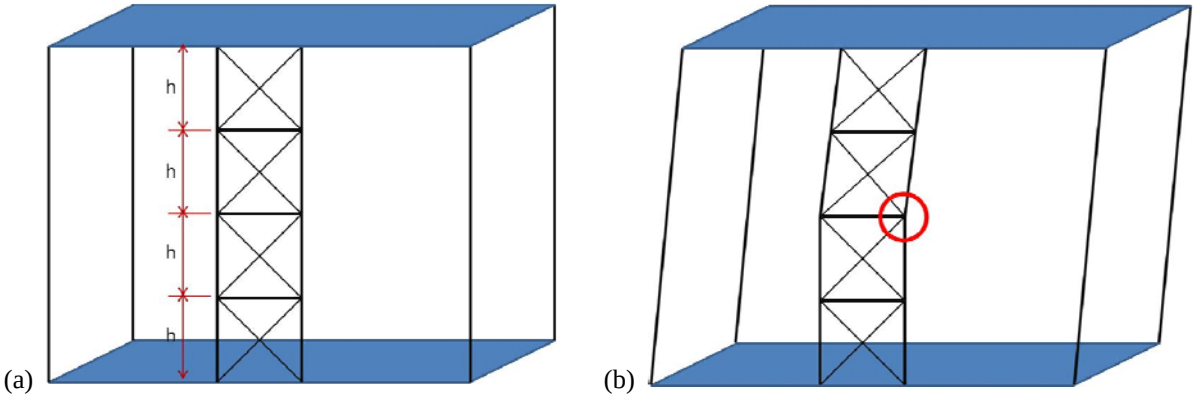

Figure 1: (a) Multitier Braced Frame Geometry; (b) Inelastic Flexural Demand in Column (Sabelli 2011)

As a first step toward quantifying the influence of weak-axis flexural yielding on the strong-axis buckling strength of multitier columns, a suite of isolated columns was designed for typical multitier braced frame loading and geometry, and studied using finite element analysis. The column designs were based on a column height of 40 ft; braced frame width of 20 ft; column dead load of 40 kips; and lateral load at the top of the multitier frame of 200 kips (Sabelli 2011). The resulting column designs and associated slenderness ratios for strong-axis buckling are listed in Table 1. All columns in the study had four tiers, similar to the frame geometry in Fig. 1. Slenderness ratios given in Table 1 are based on H = 40 ft.

Table 1: Columns for Computational Study

Column Size	$(KL/r)_x$ for H = 40’
W12x65	90.9
W18x86	61.8
W24x131	47.1
W30x211	37.2

The combination of weak-axis flexure and strong-axis flexural buckling causes the neutral axis of bending to deviate from the principal axes of the cross section. As a result, the maximum compressive and tensile stresses occur on diagonally opposite corners of the wide flange cross section, while the other diagonally opposed corners of the cross-section unload elastically. This unsymmetrical stress distribution gives rise to torsional as well as flexural deformation. Thus, torsional restraint at the tier levels of multitier braced frame columns is an important consideration.

2. Finite Element Model

To study the effect of weak-axis flexural yielding on strong-axis buckling strength, a three-dimensional finite element model of an isolated column was developed using the *Abaqus FEA* software package (Simulia 2011). Fig. 2 illustrates the finite element model for a multitier column with four tiers. The columns were modeled with four-node shell elements with full

integration. Geometric nonlinearities were incorporated in the models through use of a large-displacement formulation.

Material nonlinearities were incorporated through the von Mises yield criterion with associated flow rule and isotropic strain hardening. The nonlinear behavior for the material was taken from tension tests of ASTM A992 steel, performed at the University of Illinois at Urbana-Champaign (Stoakes and Fahnestock 2012). The Cauchy stress vs. logarithmic strain data used in the analyses is illustrated in Fig. 3. As shown in Fig. 3, the flanges and webs were assigned different yield stresses, but similar strain hardening behavior, based on the tension test results.

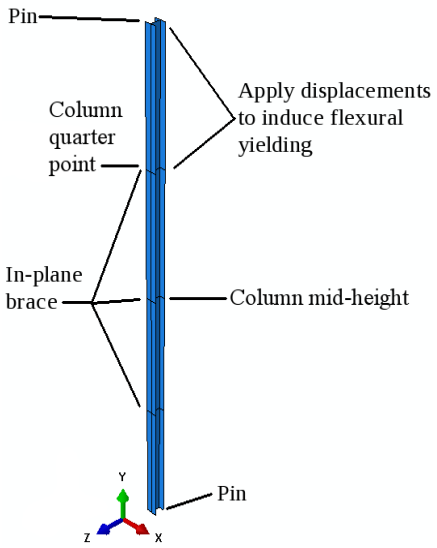

Figure 2: Finite Element Model Geometry

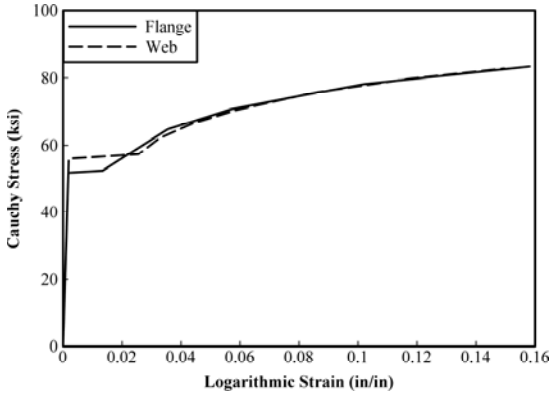

Figure 3: Cauchy Stress vs. Logarithmic Strain for ASTM A992 Wide Flange Column

Since the FEA model consisted of a single column from a multitier braced frame model, the interaction between the column and the intermediate beams at the tier levels was simulated with appropriate boundary conditions. At the bottom of the column, the three translational degrees-of-freedom (dofs) were fixed. At the top of the column, the x-direction and z-direction translational dofs were fixed. The y-direction was not fixed at the top of the column to allow application of a compressive load after inducing in-plane flexural yielding. In addition, rotation about the y-axis

(torsion) was fixed at the top and bottom of the column. Plane section constraints were enforced at both ends of the column, which resulted in warping restraint at these sections.

At the three intermediate weak-axis brace points (tier levels), two different torsional restraint conditions were considered owing to the importance of torsional deformations. In one case, the x-direction translational dofs were fixed at all points in the web at the cross section. This provided a rigid torsional restraint at each tier level in addition to preventing translational displacement. This case is illustrated in Fig. 4 and is called torsion restrained (TR). In the second case, the x-direction translational dofs were fixed at a group of nodes along the centerline of the column. This restraint condition prevented translation, but allowed torsional deformation, which is equivalent to the restraint provided by a vertical shear tab connection between the column and the intermediate beams. This case is illustrated in Fig. 5 and is called torsion free (TF).

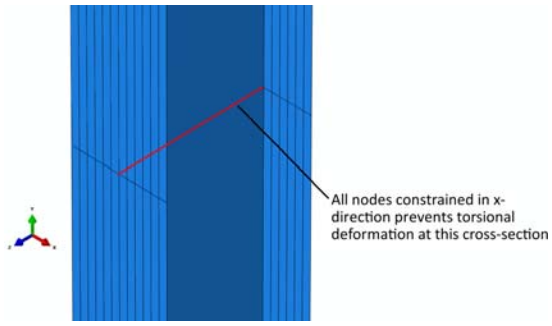

Figure 4: Intermediate Brace Point with Torsional Restraint (TR Cases)

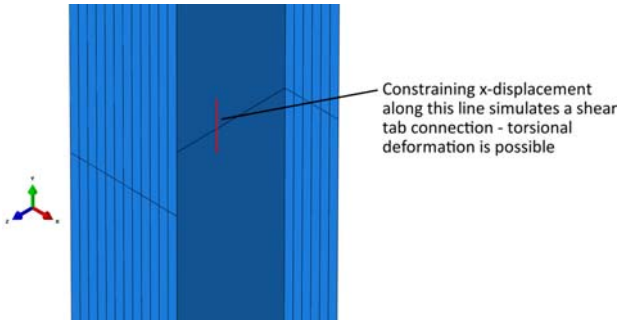

Figure 5: Intermediate Brace Point without Torsional Restraint (TF Cases)

Weak-axis flexural yielding was induced in the column by displacing the top of the column and the first brace point, for weak-axis flexural yielding at column mid-height, or only the top of the column, for weak-axis flexural yielding at a column quarter point. The locations of weak-axis flexural yielding were noted in Fig. 2. In-plane rotations of 0.00 rad, 0.01 rad, 0.02 rad, 0.03 rad, and 0.04 rad were investigated. The 0.00 rad in-plane rotation case was used to validate the finite element models. After inducing the prescribed in-plane rotation, a compressive load was applied to the top of the column. The Riks arc-length technique (Simulia 2011) was used to trace column behavior after the critical buckling load was reached.

2.1 Geometric Imperfections

Geometric imperfections were specified for the in-plane (weak-axis) and out-of-plane (strong-axis) directions of the columns. The imperfection geometry was based on eigenvalue buckling analyses of the columns and the imperfection magnitude was based on the AISC *Code of*

Standard Practice for Steel Buildings and Bridges (AISC 2005a). In the out-of-plane direction, the column was considered to have a maximum out-of-straightness equal to *H*/1500, which is the maximum out-of-straightness permitted for rolled wide flange shapes. In addition, this value equals the out-of-straightness assumed in development of the AISC *Specification* column curve (AISC 2005c). In the in-plane direction, the column was assumed to have a maximum out-of-straightness equal to *h*/1000 for each tier, which is the maximum out-of-straightness permitted between column brace points. The geometric imperfections are illustrated in Fig. 6.

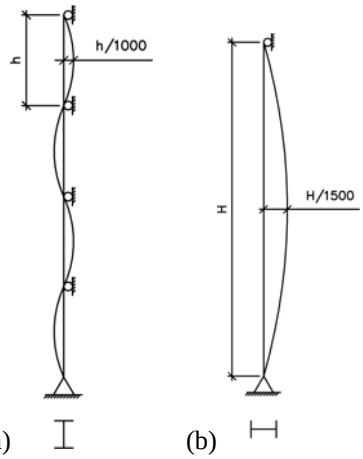

Figure 6: Geometric Imperfections: (a) In-Plane; (b) Out-of-Plane

2.2 Residual Stresses

In addition to geometric imperfections, residual stresses were included in the finite element models. The Lehigh residual stress pattern (Galambos and Ketter 1958) was used to determine the magnitudes of the residual normal stresses in the flanges and webs of the columns. To implement the residual stress pattern in the column flanges, the flanges were partitioned into strips across their width and temperature changes were applied to each of the strips to induce the appropriate residual stress. The stress pattern and flange discretization are shown in Fig. 7.

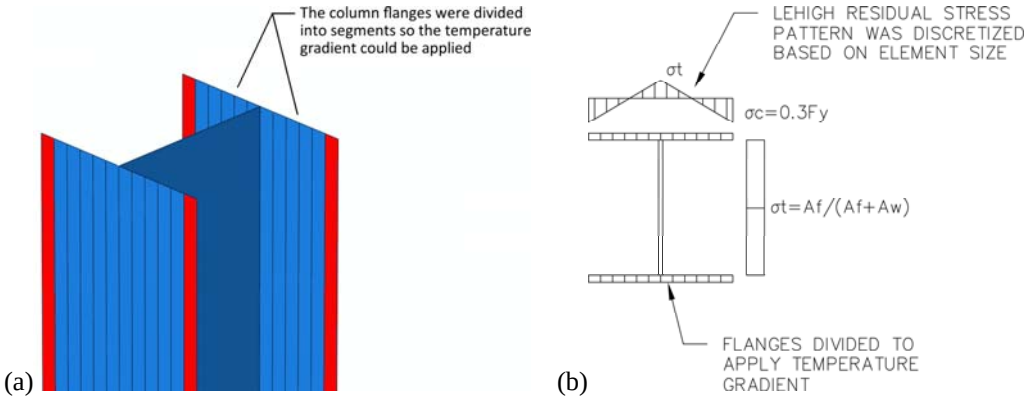

Figure 7: Residual Stress: (a) Flange Discretization; (b) Residual Stress Pattern

3. Results

The finite element models were validated by comparing the computationally predicted compressive strength for no in-plane rotation to the nominal buckling strength from the AISC *Specification* (2005c). Fig. 8 shows compressive load vs. mid-height deflection data for the

columns with no rad in-plane rotation as well as the nominal buckling strength values for the strong axis. Based on these results, the finite element models were deemed acceptable for the present study.

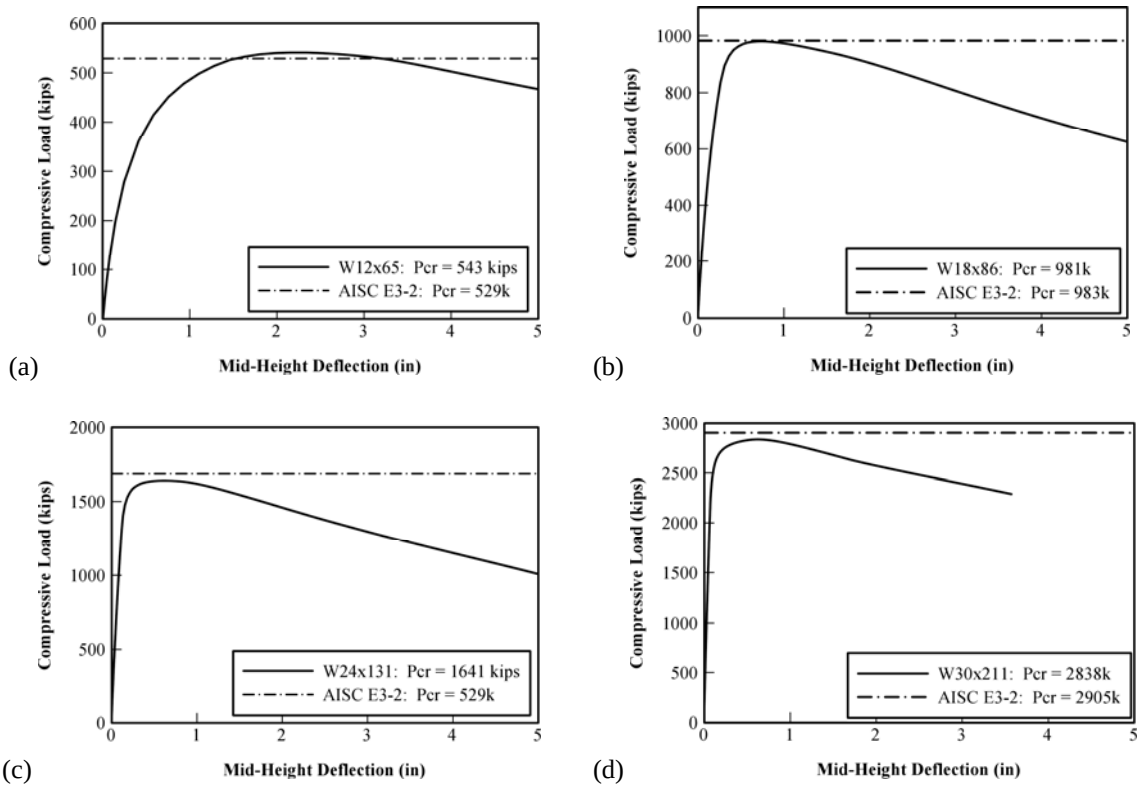

Figure 8: Validation of Finite Element Models: (a) W12x65; (b) W24x131; (c) W24x131; (d) W30x211

After validating the models, each column was subjected to in-plane flexural rotation at column mid-height. Fig. 9 illustrates the compressive load vs. mid-height deflection data for each of the columns with torsion-free boundary conditions at the tier levels. Results for no in-plane rotation are given by a solid line and the remaining line types denote in-plane column rotations ranging from 0.01 to 0.04 rad. The percent difference from the critical buckling load for no in-plane rotation is given in parentheses in the legends in Fig. 9.

In the Fig. 9 caption, the column designation includes an abbreviated description of the column boundary conditions and loading. A ‘TF’ after the column name indicates torsion free tier boundary conditions and ‘mid’ indicates in-plane flexural yielding was induced at mid-height of the column.

The results shown in Fig. 9 clearly demonstrate that the strong-axis buckling strength of multitier wide flange columns, which are not torsionally braced at the tier levels, is significantly degraded by the presence of weak-axis flexural yielding. An in-plane rotation of 0.01 rad resulted in buckling strength loss of 5 to 9%. In addition, when in-plane rotations of 0.04 rad were imposed, the buckling strength loss was 17 to 32%. In general, deeper columns demonstrated lower decreases in buckling strength after in-plane flexural yielding, but this is likely due to their larger

torsional stiffness. Larger mid-height deflections at the critical buckling load were also an outcome of in-plane flexural yielding.

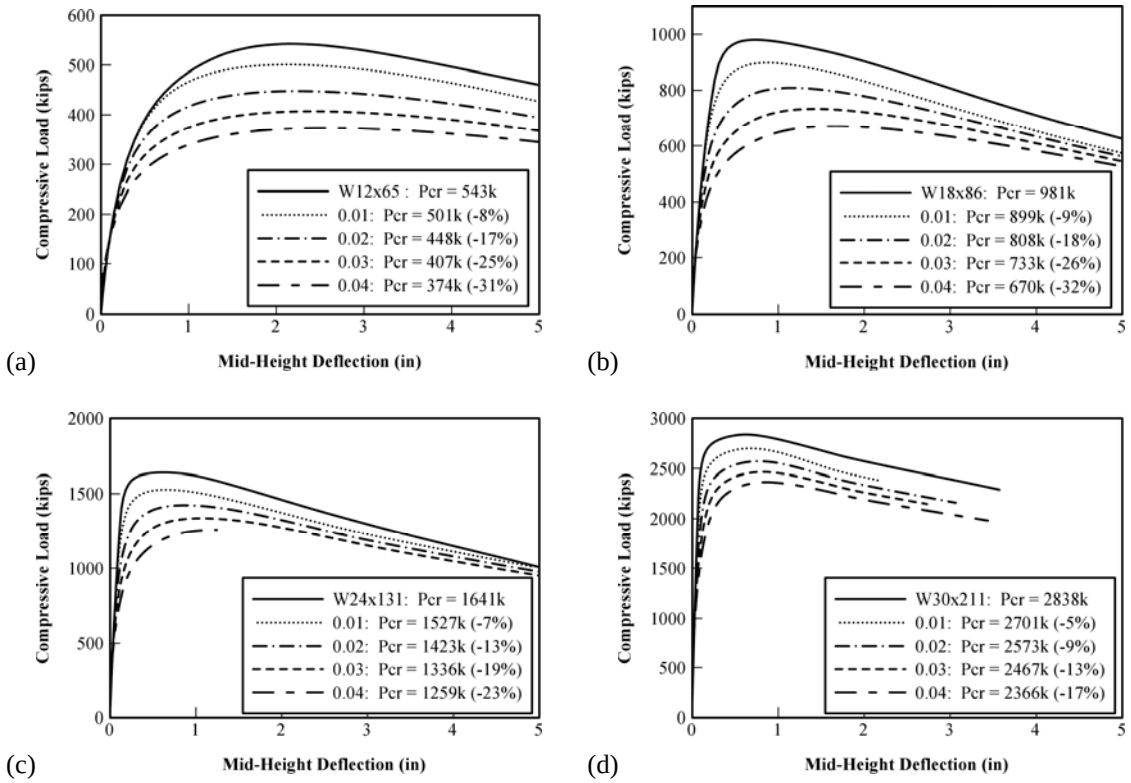

Figure 8: Compressive Load vs. Mid-Height Deflection: (a) W12x65_TF_mid; (b) W18x86_TF_mid; (c) W21x131_TF_mid; (d) W30x211_TF_mid

If torsional restraint is provided at the tier levels, however, the reduction in buckling strength is less severe. Fig. 10 illustrates compressive load vs. mid-height deflection for a W18x86 column with torsional restraints at the tier levels. The 'TR' abbreviation in the figure caption denotes this change.

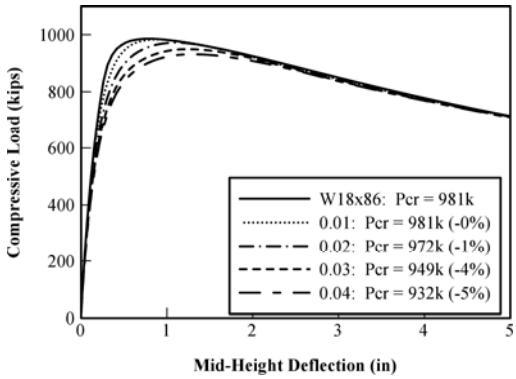

Figure 10: Compressive Load vs. Mid-Height Deflection for W18x86_TR_mid

In this case, in-plane rotation of 0.04 rad resulted in buckling strength reduction of only 5%. In addition, the mid-height deflection at the critical buckling load was less than the TF cases. The

buckling strength reductions for the remaining columns with TR tier boundary conditions were similar.

In addition to the effect of tier boundary conditions, the location of weak-axis flexural yielding was also varied to study its effect on strong-axis buckling strength. Fig. 11 illustrates the compressive load vs. mid-height deflection for a W18x86 column with the weak-axis flexural yielding located at a column quarter point. The 'qrtr' abbreviation in the figure caption denotes the location of the flexural yielding. Torsion free tier boundary conditions were used in this case since the results presented above demonstrated it was more severe than TR tier boundary conditions.

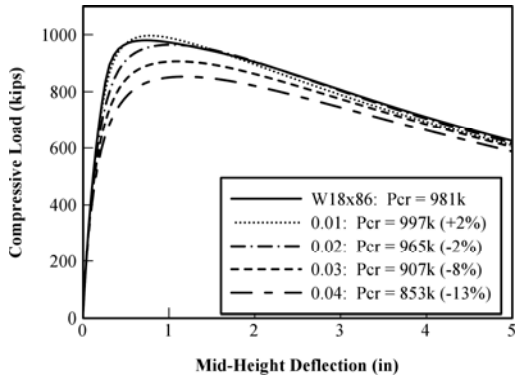

Figure 11: Compressive Load vs. Mid-Height Deflection for W18x86_TF_qrtr

Fig. 11 demonstrates that if in-plane flexural yielding occurs at a column quarter point, the reduction in buckling strength is significantly lower than when the yielding occurs at column mid-height. For the W18x86 column, when an in-plane rotation of 0.04 rad was achieved at a column quarter point, the buckling strength decreased only 13%, compared to 32% for a W18x86 with in-plane rotation at column mid-height. Fig. 11 also shows that buckling strength increased for an in-plane rotation of 0.01 rad. In this instance, the in-plane rotation straightened the weak-axis imperfections, which resulted in the buckling strength increase. The buckling strength reductions for the remaining columns with weak-axis flexural yielding at a column quarter point and TF tier boundary conditions were similar.

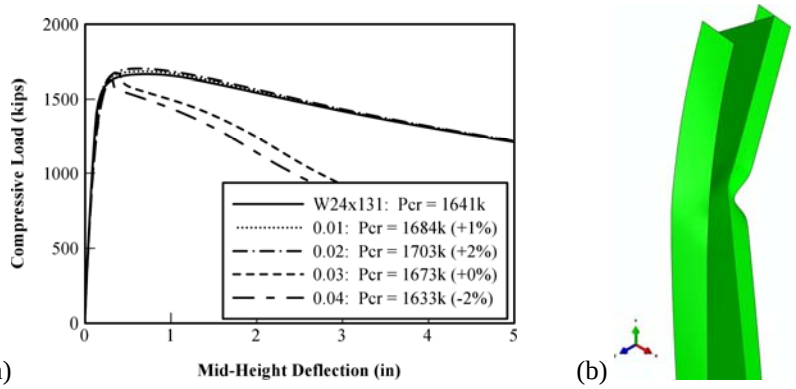

Figure 12: W24x131_TR_qrtr: (a) Compressive Load vs. Mid-Height Deflection; (b) Flange Local Buckling

While the behavior of the W12x65 column and W30x211 column with TR tier boundary conditions were similar to the W18x86 column for weak-axis flexural yielding at a column quarter point, the behavior of the W24x131 with TR tier boundary conditions was markedly different. Fig. 12 illustrates the compressive load vs. mid-height deflection data for this case.

Fig. 12a shows that after reaching ultimate buckling load at in-plane rotations of 0.03 and 0.04 rad, the strength of the W24x131 decreased rapidly. This was due to local buckling of the column flanges, which is illustrated in Fig. 12b. This behavior suggests that deep multitier columns may be susceptible to local buckling even though they have compact cross-sections. Local buckling was not observed in any other simulation.

4. Conclusions and Future Research

This paper presented research on the flexural buckling behavior of wide flange columns in multitier braced frames. A multitier braced frame is created when a braced frame with a large aspect ratio is subdivided into smaller frames with intermediate beams. Out-of-plane bracing at the tier levels is not provided, however. During a large seismic event, inelasticity in the braces can lead to differential tier drifts that induce weak-axis flexural yielding of the columns. This inelasticity is not accounted for in current column strength curves. Three-dimensional finite element models of isolated columns were created and subjected to various magnitudes of in-plane flexural stresses at column mid-height and at a column quarter-point. The effect of tier-boundary conditions, torsion free or torsion restrained, was also investigated.

The results from the computational studies suggest that strong-axis buckling strength of multitier columns, without torsional restraint at the tier levels, is reduced in the presence of weak-axis flexural yielding. The buckling strength decreased by 5 to 9% for in-plane rotations of 0.01 rad and 17 to 32% for in-plane rotations of 0.04 rad. This restraint condition represents vertical shear tab connections between the beams and columns in a multitier braced frame. Providing torsional restraint at the tier level substantially improves column performance, although reductions in the strong-axis buckling strength on the order of 5% were noted. These observations were noted for columns with weak-axis flexural yielding at column mid-height.

When weak-axis flexural yielding was induced at a column quarter-point, the reduction in strong-axis buckling strength was not as severe as when yielding occurred at column mid-height, but reductions on the order of 10% were still observed. In addition, local flange buckling was noted for one column when subjected to weak-axis flexural yielding at a column quarter-point. The reduction in the critical buckling load was negligible, but the column strength degraded rapidly after the critical buckling load was achieved.

Future research on this topic will focus on three areas. First, a wider array of isolated columns needs to be studied. The behavior of columns with non-compact or slender elements has not been investigated and the behavior of columns with similar flexural buckling properties, but different torsional properties, also needs to be explored. Second, finite torsional restraint at the tier levels that varies between torsion free and torsion fixed needs to be considered. Finally, the present study focused solely on isolated columns, but the interaction between a column and the other members of a multitier braced frame during a seismic event needs to be investigated through

finite element analysis. These analyses would capture realistic column loading conditions and simulate torsional deformation of the column due to out-of-plane buckling of the braces.

Acknowledgments

This research was developed with guidance from AISC Task Committee 9 – Seismic Design, which is chaired by James Malley. The advice and input from Rafael Sabelli are particularly appreciated. All opinions, findings and conclusions are those of the authors.

References

American Institute of Steel Construction (2005a). *Code of Standard Practice for Steel Buildings and Bridges*, AISC 303-05, Chicago, Illinois, 69 pp.

American Institute of Steel Construction (2005b). *Seismic Provisions for Structural Steel Buildings*, ANSI/AISC 341-05, Chicago, Illinois, 330 pp.

American Institute of Steel Construction (2005c). *Specification for Structural Steel Buildings*, ANSI/AISC 360-05, Chicago, Illinois, 256 pp.

Galambos, T.V. and Ketter, R.L. (1958). *Columns Under Combined Bending and Thrust.*, Fritz Engineering Laboratory Report 205A.21, Bethlehem, Pennsylvania.

Sabelli, R., 2011. Personal communication.

Simulia (2011). *Abaqus FEA*, www.simulia.com.

Stoakes, C.D. and Fahnestock, L.A. (2012). "Cyclic flexural analysis and behavior of beam-column connections with gusset plates." *J. Const. St. Res.*, accepted for publication.